Tamarind pod shell (*Tamarindus indica* L.) as biosorbent to remove zinc (II) ions from aqueous solution

[1]Jagruti S. Vaza, [2]Satish A. Bhalerao

Environmental Sciences Research Laboratory,
Department of Botany,
Wilson College, Mumbai-400007, Affiliated to University of Mumbai, M. S., India.

***Abstract*: Removal of the Zn (II) metal ions from aqueous solution was carried out using tamarind pod shell powder (*Tamarindus indica* L.). The biosorbent was characterized by Fourier transmission infrared, scanning electron microscope and X-ray difractometer techniques. The effect of solution pH, adsorbent dose and initial concentration of metal solution, contact time, agitation speed and temperature was investigated in a systematic manner. Experimental data were analyzed by kinetic parameters such as pseudo-first order and pseudo-second order models and found that the biosorption of Zn (II) followed pseudo-second order model by its good correlation coefficient values which are very close to the unity. The equilibrium data were analyzed by using Langmuir, Freundlich, Dubnin– Radushkevich isotherm models. Among these isotherm models Freundlich model was fitted well with its good correlation coefficient values. The results concluded that the Tamarind pod shell powder (*Tamarindus indica* L.) was an efficient, eco-friendly, and economically low cost adsorbent in the removal of Zn (II) ions from the aqueous medium.**

***Keywords*: Tamarind pod shell (*Tamarindus indica* L.), Zinc (II), Adsorption isotherm, adsorption kinetics.**

Introduction

Excessive release of heavy metals into the environment due to industrialization and urbanization poses great problem worldwide. Unlike organic pollutants, the majority of which are susceptible to biological degradation, heavy metal ions do not degrade into harmless end products (Gupta *et al*., 2001). It adversely affects human life through water resources, agriculture and biological products (Naidu *et al*., 1996). Heavy metals pose a significant threat to the environment and public health because of their toxicity, accumulation in the food chain and persistence in nature. In order to minimise the risk of environmental pollution from the waste effluents containing high concentrations of heavy metals, it is necessary to develop new techniques for metal removal from aqueous solutions.

Zinc is the fourth among metals of the world in annual consumption. It is extensively used in the automobile industry, for the production of protective coatings for iron and steel, in cosmetics, powders, ointments, antiseptics, paints, varnishes, rubber and linoleum. Zinc is also needed for manufacturing of parchment papers, glass, automobile tires, television screens, dry cell batteries and electrical equipment. The main sources of Zn in the environment are zinc fertilizers, sewage sludges and mining and smelting (Bradl *et al*., 2005). The average human body contains about 2 grams of zinc, which is essential for the normal activity of DNA polymerization and for protein synthesis. Soluble and astringent acid salts, such as ZnSO4 in large doses (about 10 g), have caused internal organ damage and death (Gupta and Sharma, 2003).

Biosorption is a physico-chemical adsorption whereby metal ions become attached to the biomass surface (Drake *et al*., 1996). The ability to adsorb metals has been investigated for many materials, including wool, rice, straw, coconut husks, peat moss (Macchi *et al*., 1986), fungi (Mueler *et al*., 1992), algae (Carvalho *et al*., 1995) and yeast (Dostalek *et al*., 2004).
In this present study, Tamarind pod shell (Tamarindus indica L.) is tried for the removal of Zinc (II). It is belongs to Fabaceae family and subfamily Caesalpinioideae. It is lowcost biomaterial and easily available.

MATERIALS and METHODS

Chemicals and reagents

All the chemicals and reagents used were of analytical reagent (AR) grade. Double distilled water was used for all experimental work including the preparation of metal solutions. The desired pH of the metal ion solution was adjusted with the help of dilute hydrochloric acid and dilutes sodium hydroxide.

Preparation of Zinc (II) solution

The stock solution of 1000 ppm of Zinc (II) was prepared by dissolving 0.1 g of zinc metal (AR grade) in 100 ml of double distilled water and further desired test solutions of zinc (II) were prepared using appropriate subsequent dilutions of the stock solution.

Preparation of biosorbent

The tamarind pod shell (*Tamarindus indica* L.) was collected and washed with several times with distilled water to remove the surface adhered particles, dirt, other unwanted material & water soluble impurities and water was squeezed out. The washed biosorbent was then dried at sunlight and grounded in a mechanical grinder to form a powder. The powder was sieved and a size

fraction in the range of 100-200 µm will be used in all the experiments. So prepared tamarind pod shell powder were used for further studies. Biomass was stored in air tighten plastic bottle to protect it from moisture.

Instrumentation:

The pH of the solution was measured by digital pH meter (EQUIP-TRONICS, model no. Eq-610) using a combined glass electrode. The concentration of zinc (II) in the solution before and after equilibrium was determined by measuring absorbance using Inductively Coupled Plasma Atomic Emission Spectroscopy (ICP-AES) technique. Biosorbent was characterized by Fourier Transform Infrared (FTIR), Scanning Electron Microscope (SEM) and X-ray diffraction (XRD).

Characterization of biosorbent by Fourier Transform Infrared (FTIR) analysis

The Fourier Transform Infrared (FTIR) spectroscopy was used to identify the functional groups present in the biosorbent. The biomass samples were examined using FTIR spectrometer (model:FT/IR-4100typeA) within range of 4004000 cm-1. All analysis was performed using KBr as back ground material. In order to form pellets, 0.02 g of biomass was mixed with 0.3 g KBr and pressed by applying pressure.

Characterization of biosorbent by Scanning Electron Microscope (SEM) analysis

The Scanning Electron Microscope (SEM) was used to see the porosity of the biosorbent. The samples were covered with a thin layer of gold and an electron acceleration voltage of 10 KV was applied and then Scanning Electron Micrograph was recorded.

Characterization of biosorbent by X-ray diffraction analysis (XRD) analysis

X-ray diffraction (XRD) was used for the qualitative and quantitative determination of solid samples of biosorbent. It works on the principle that X-ray diffraction pattern is unique for each sample. This pattern from XR-D was compared with a known compound and the chemical compound was identified.

Experimental procedure

The static (batch) method was employed at temperature (30^0C) to examine the biosorption of zinc (II) by biosorbent. The method was used to determine the biosorption capacity, stability of biosorbent and optimum biosorption conditions. The parameters were studied by combining biosorbent with zinc (II) solution in 250 ml separate reagent bottles. The reagent bottles were placed on a shaker with a constant speed and left to equilibrate. The samples were collected at predefined time intervals, centrifuged, the content was separated from the biosorbent by filtration, using Whatmann filter paper and amount of zinc (II) in the filtrate solutions was determined by Inductively Coupled Plasma-Atomic Emission Spectroscopy (ICP-AES). The following equation was used to compute the percent removal (% Adsorption) of zinc (II) by the biosorbent,

$$\% \text{ Ad} = \frac{(C_i - C_e)}{C_i} \times 100 \qquad \textbf{(1)}$$

Where *Ci* and *Ce* are the initial concentrations and equilibrium concentrations of the zinc (II) in mg/L.

The equilibrium adsorptive quantity (qe) was determined by the following equation,

$$q_e = \frac{(C_i - C_e)}{w} \times V \qquad \textbf{(2)}$$

Where q_e (mg metal per g dry biosorbent) is the amount of zinc (II) biosorbed, V (in liter) is the solution volume and w (in gram) is the amount of dry biosorbent used.

Desorption study:

To evaluate desorption efficiency; zinc (II) loaded biosorbent was dried after equilibrium sorption experiments. The dried biosorbent was contacted with 0.1 M nitric acid (HNO3), 0.1 M hydrochloric acid (HCl) and 0.1 sulphuric acids (H_2SO_4) separately for 1 hour to allow zinc (II) to be release from biosorbent. The samples were separated from the biosorbents by filtration, using Whitman filter paper and amount of and zinc (II) in the filtrate solutions was determined to find out desorption efficiency. Desorption efficiency was calculated from the amount of metal ions adsorbed on the biosorbent and the final metal ion concentration in the biosorption medium (equation 3)

$$\textit{Desorption efficiency}\ (\%) = \frac{\text{released metal ions in mg/L}}{\text{initially adsorbed metal ions in mg/L}} \times 100 \qquad \textbf{(3)}$$

RESULTS AND DISCUSSION

Characterization of biosorbent by Fourier Transform Infrared (FTIR) analysis

To investigate the functional groups of biosorbent and metal loaded with biosorbent, a FTIR analysis was carried out and the spectra are shown in Figure.1. (a and b). As seen in the figure unloaded biomass displays a number of absorption peaks, reflecting the complex nature of biomass. The broad peak at 3422 cm^{-1} is the indicator of -OH and -NH groups. The peaks at 2366 cm^{-1} and 2345 cm^{-1} are stretching peaks. The peaks located at 1734 cm^{-1} and 1617 cm^{-1} are characteristics of carbonyl group. The presence of -OH group along with carbonyl group confirms the presence of carboxyl acid groups in the biomass. The peak at 1508 cm^{-1} is associated

with the stretching in aromatic rings. The peaks observed at 1078 cm^{-1} are due to C-H and C-O bonds. The –OH, NH, carbonyl and carboxyl groups are important sorption sites. As compared to simple biosorbent, biosorbent loaded with zinc (II) ions, the broadening of -OH peak at 3447 cm^{-1} and carbonyl group peak at 1734 cm^{-1} and 1617cm^{-1} was observed. This indicates the involvement of hydroxyl and carbonyl groups in the biosorption of zinc (II).

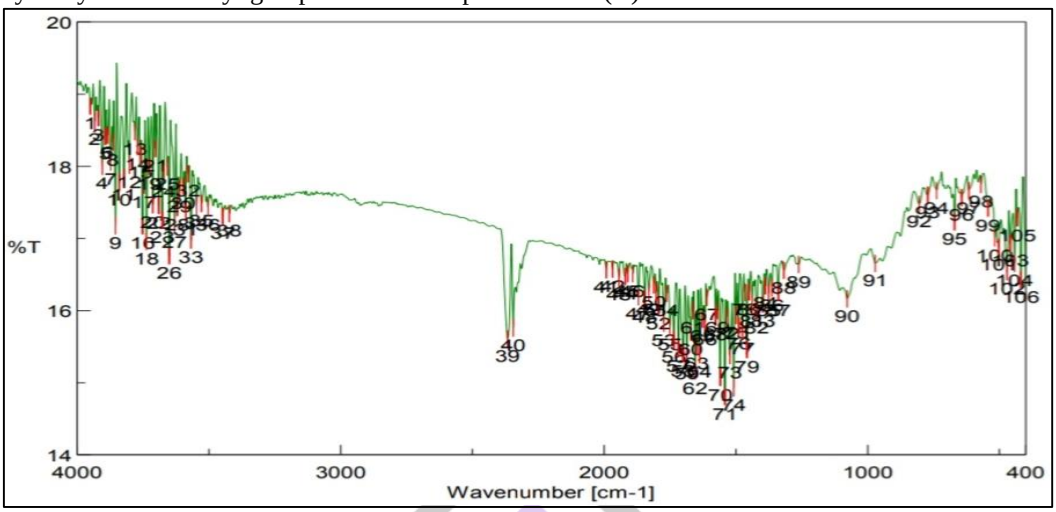

(a)

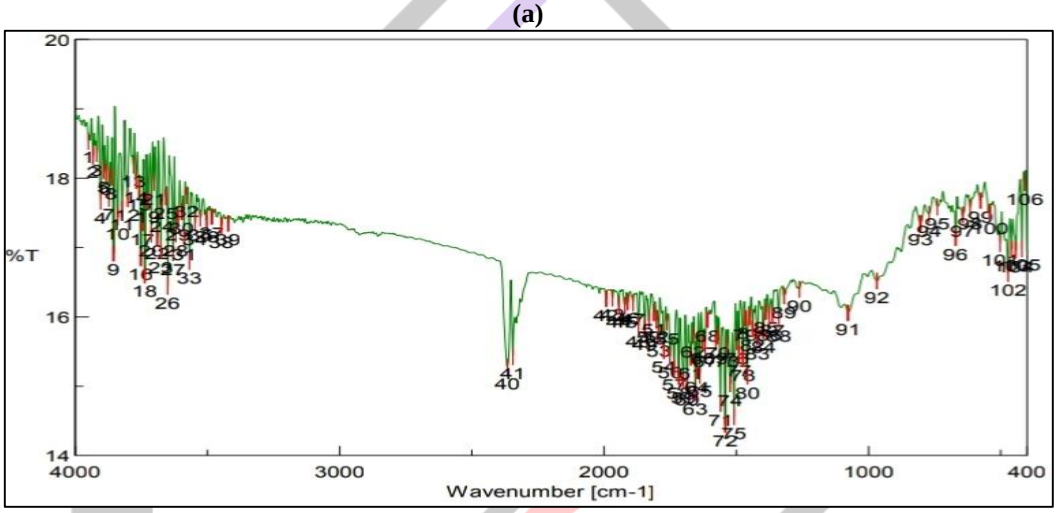

(b)

Figure.1. FTIR spectra (a) biosorbent tamarind pod shell (*Tamarindus indica* L.) (b) biosorbent tamarind pod shell (*Tamarindus indica* L.) loaded with zinc (II)

Characterization of biosorbent by Scanning Electron Microscope (SEM) analysis

The surface characteristics, structure and particle size distribution of biosorbent before and after biosorption was examined using Scanning Electron Microscope (SEM). The SEM micrographs are shown in Figure. 2. (a and b). These micrographs represent a porous structure with large surface area. The SEM clearly demonstrated that there is more uniformity after biosorption on metal ions in comparison to before biosorption. It was evident from the mictrographs that the biosorbent presents an unequal structure before metal adsorbed. The number of canals in the biosorbent was higher in the initial case. The metal ions adsorbed on the cell wall matrix and created stronger cross linking and uniformity on the surface of biosorbent.

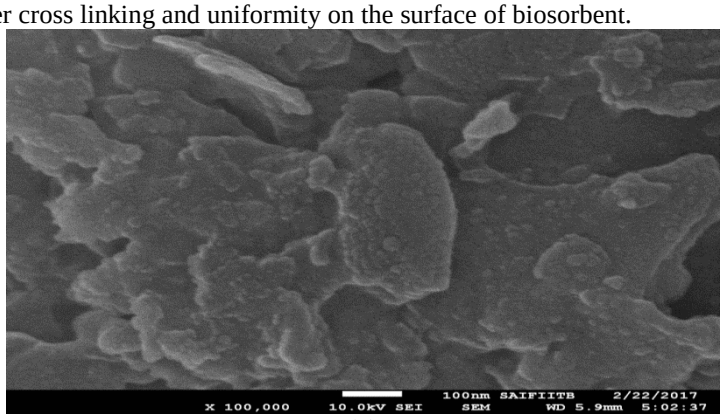

(a)

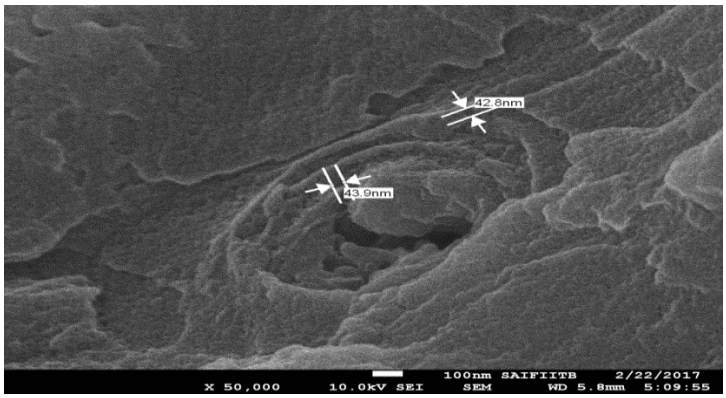

(b)

Figure. 2. SEM analysis (a) biosorbent tamarind pod shell (*Tamarindus indica* L.) unloaded with zinc (II) ions (b) biosorbent tamarind pod shell (*Tamarindus indica* L.) loaded with zinc (II) ions

Characterization of biosorbent by X-ray diffraction analysis (XRD) study

XRD pattern of the tamarind pod shell (*Tamarindus indica* L.) before biosorption of zinc (II) solution is shown in Figure 3 (a). Broad peaks were obtained instead of sharp peaks indicating the sample was poorly crystalline. The XRD spectra of after biosorption of zinc (II) exhibit strong peaks at 2θ value of 20.14º, 30.08º and 52.52º equivalent to 381.638, 266.772 and 115.385 respectively for tamarind pod shell (*Tamarindus indica* L.). Figure 3 (b) represents the XRD pattern of zinc (II) loaded plant materials.

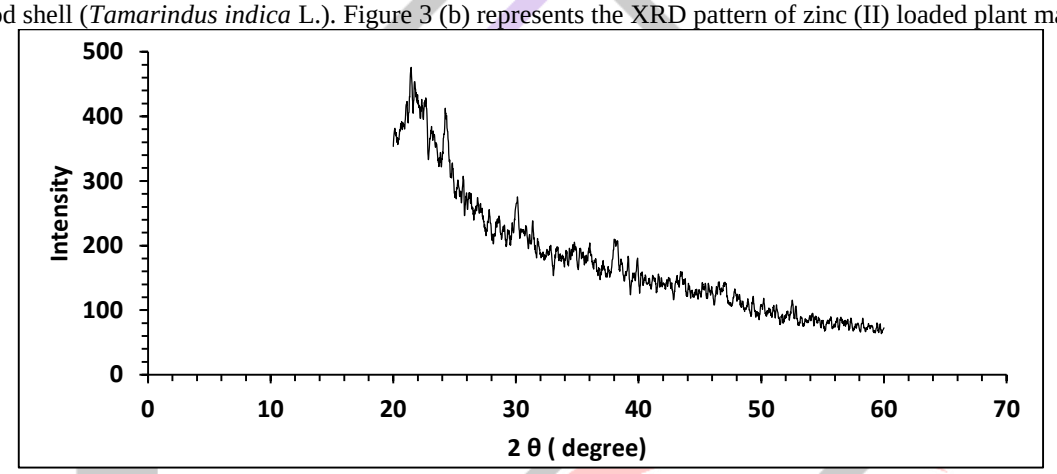

(a)

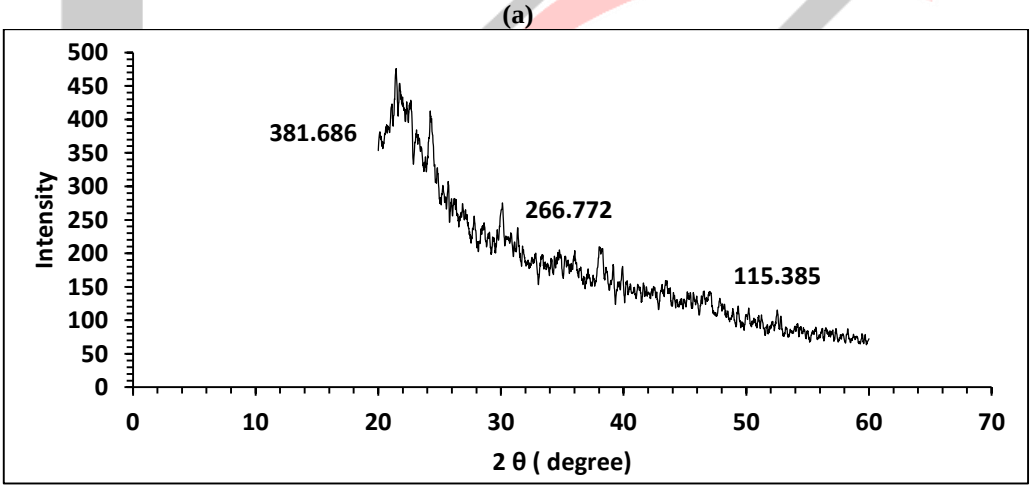

(b)

Fig.3: X-ray diffraction analysis (XR-D) study (a) Biosorbent tamarind pod shell (*Tamarindus indica* L.) (b) Biosorbent tamarind pod shell (*Tamarindus indica* L.) loaded with zinc (II)

Effect pH

The Batch equilibrium studies at different pH are studied from the range 2-9. They are presented in the Fig. 4. The graph is plotted using percentage of metal uptake mg/L to initial pH. The solution pH is one of the important variables governing biosorption materials by sorbents. It is found that the uptake of zinc (II) by biomass depend on pH. There is a steep increase up to pH 6 after that there is a gradual decrease, as seen in the graph. It is interesting to note that tamarind pod shell powder (*Tamarindus indica* L.)

adsorbed zinc (II) at pH 6 is very high. The result shows adsorption of biomass depends on pH of medium. So pH 6 is optimized for this batch equilibrium studies.

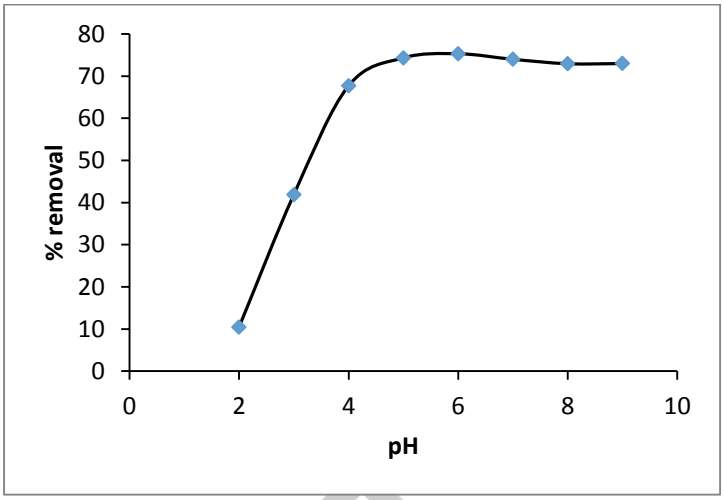

Fig.4: Effect of pH on zinc (II) biosorption by tamarind pod shell (*Tamarindus indica* L.) (biosorbent dose concentration: 5 g/L, zinc (II) concentration: 5 mg/L, contact time: 120 minutes, temperature: 30^{0}C, agitation rate 120 rpm)

Effect on biosorbent dose

The effect of solid to liquid ratio on the zinc (II) was studied by keeping all other parameters constant ranging from 1 g/L to 15 g/L. This range of biosorbent dose is used to determine the suitable quantity of biomass for maximum sorption. The graph is plotted for percentage removal efficiency against biosorbent dose is shown in the Fig. 5 for the biomass tamarind pod shell powder (*Tamarindus indica* L.). It is evident from the graph that an adsorbent dose 5 g/L is sufficient to removal of zinc (II) metal by the biomass. From the observations it is interesting to note that further increment in sorbent did not cause significant improvement in the sorption.

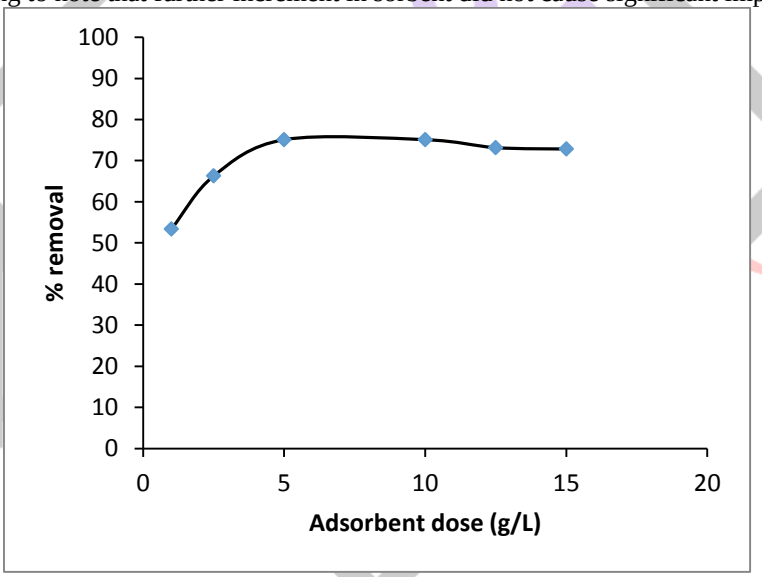

Figure 5: Effect of biosorbent dose concentration on zinc (II) biosorption by tamarind pod shell (*Tamarindus indica* L.) (pH: 6, initial zinc (II) concentration: 5 mg/L, contact time: 120 minutes, agitation rate: 120 rpm, temperature: 30^{o}C)

Effect of contact time

Contact time is maximum time taken by the sorption experiment to achieve equilibrium after which no further metal uptake is adsorbed. The results for the contact times are given in the graph is plotted for the biomasses and is shown in the Fig. 6. It can be noticed from the graph that the contact time significantly affects the metal uptake. The metal sorption increases with increasing time and attain equilibrium at 150 min according to the result. From the observation it is concluded that 150 min are sufficient for the sorption to attain equilibrium for tamarind pod shell (*Tamarindus indica* L.) biomasses.

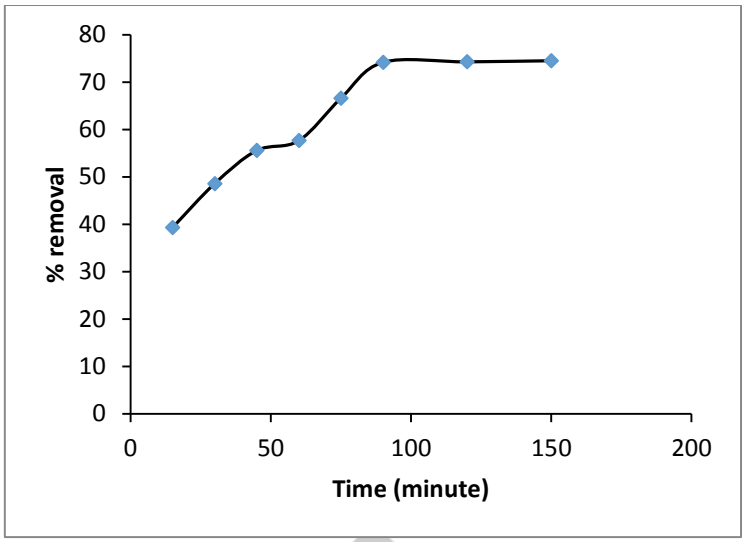

Figure 6: Effect of contact time on zinc (II) biosorption by tamarind pod shell (*Tamarindus indica* L.) (pH: 6, biosorbent dose concentration: 5 g/L, initial zinc (II) concentration: 5 mg/L, agitation rate: 120 rpm, temperature: 30^0C)

Effect of Initial metal ion Concentration:

The rate of sorption is function of initial concentration of metal ion which makes it an important factor to be considered for effective biosorbent. The initial metal ion concentrations provide driving force overcome mass transfer ions between aqueous and solid phase. The initial concentrations are changed in the range of 5 mg/L to 250 mg/L by keeping all other parameters constant. The results are shown in the Fig. 7. The sorption capacity increases with increasing initial metal ion concentration for zinc (II) for tamarind pod shell (*Tamarindus indica* L.) biomass.

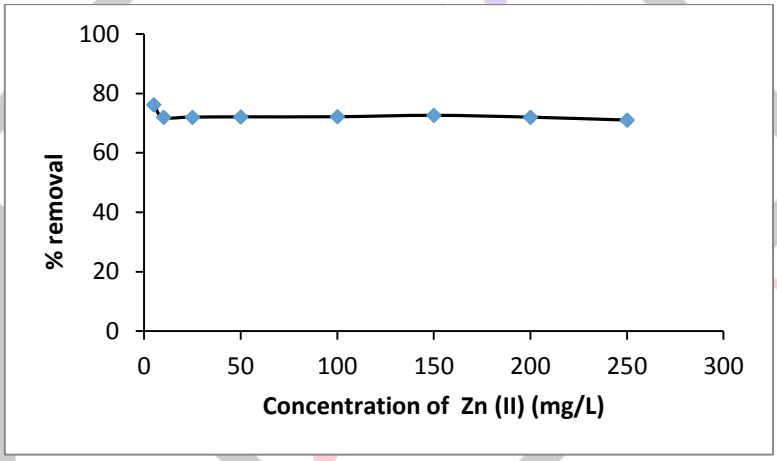

Figure 7: Effect of initial zinc (II) concentration on zinc (II) biosorption by tamarind pod shell (*Tamarindus indica* L.) (pH: 6, biosorbent dose concentration: 5 g/L, contact time: 120 minute, agitation rate: 120 rpm, temperature: 30^0C)

Effect of temperature:

Effect of temperature on removal of zinc (II) from aqueous solutions using tamarind pod shell was studied at different temperatures from 20^0C-40^0C. The influence of temperature is depicted in Figure 8. Maximum sorption was seen at 30^0C with percentage removal 75.18%.

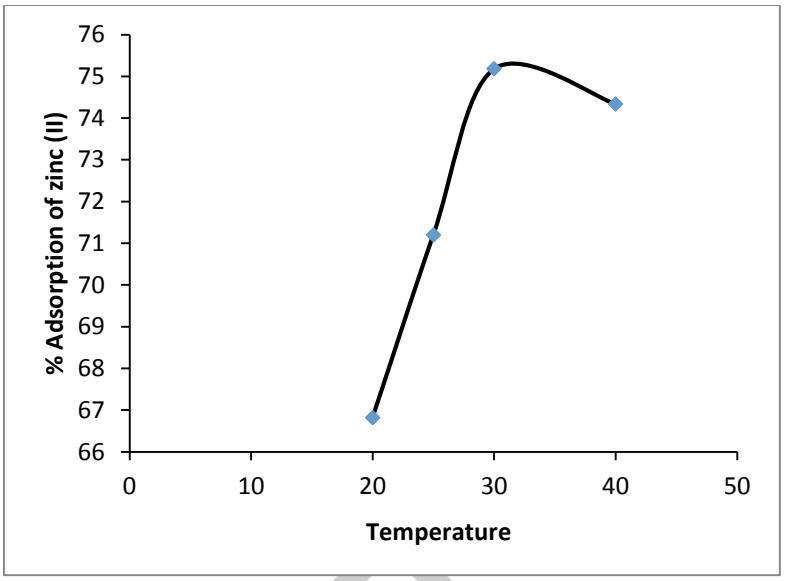

Figure 8: Effect of temperature on zinc (II) biosorption by tamarind pod shell (*Tamarindus indica* L.) (pH 6.0, biosorbent dose concentration: 5 g/L, agitation rate: 120 rpm, initial zinc (II) concentration: 5 mg/L, contact time: 120 minutes.)

Effect of stirring speed:

The stirring speed also influenced the biosorption process (Fig. 9). Agitation speed takes part in the contact between the metal ions and the biomass and influences the mass transfer in system sorbent-sorbat. Higher metal uptake and recovery of 75.31% were at 120 rpm. (Selatnia *et al*., 2004) explained the lower metal uptake at higher agitation speeds with the non-homogeneity of the sorbent-sorbat system as a result of vortex phenomena.

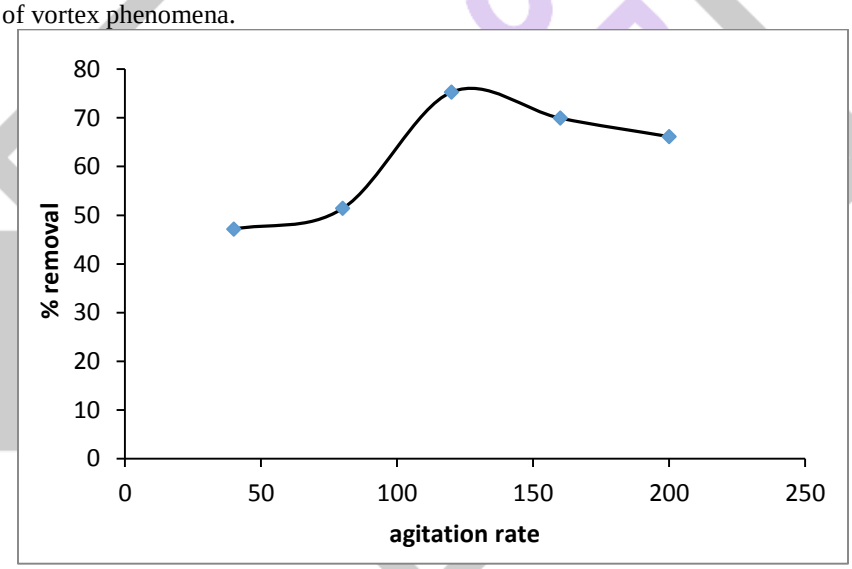

Figure 9: Effect of stirring speed on zinc (II) biosorption by tamarind pod shell (*Tamarindus indica* L.) (pH: 6, biosorbent dose concentration: 5 g/L, initial zinc (II) concentration: 5 mg/L , contact time: 120 minute, temperature: 30^0C)

Desorption study

In application of real wastewater, desorption of heavy metal ions in the biosorbent is important process. Tamarind pod shell (*Tamarindus indica* L.) was the most effective waste biosorbent with desorption efficiency 71.76% (0.1 M nitric acid), 47.58% (0.1 M hydrochloric acid) and 56.77% (0.1 M sulphuric acid). Nitric acid has shown highest desorbed capacity of zinc (II) followed by hydrochloric acid and sulphuric acid from Tamarind pod shell (*Tamarindus indica* L.).

Adsorption Isotherm

The analysis of the adsorption isotherms data by fitting them into different isotherm models is an important step to find the suitable model that can be used for design process. The experimental data were applied to the two-parameter isotherm models: Langmuir, Freundlich, Dubinin-Kaganer-Redushkevich (DKR) and Temkin. Adsorption isotherms data for biosorption of zinc (II) by tamarind pod shell (*Tamarindus indica* L.) is shown in

The Langmuir (Langmuir, 1916) sorption model was chosen for the estimation of maximum zinc sorption by the biosorbent. The Langmuir isotherm can be expressed as

$$q = \frac{q_m\, b\, C_e}{1+bC_e} \qquad (4)$$

Where Q_{max} indicates the monolayer adsorption capacity of adsorbent (mg/g) and the Langmuir constant b (L/mg) is related to the energy of adsorption. For fitting the experimental data, the Langmuir model was linearized as

$$\frac{1}{q} = \frac{1}{q_m\, b\, C_e} + \frac{1}{q_m} \qquad (5)$$

The linear plots of 1/q vs $1/c_e$ is shown in Figure10 (a). The two constants b and q_m are calculated from the slope ($1/q_{m\cdot b}$) and intercept ($1/q_m$) of the line. The values of q_m, b and regression coefficient (R^2) are listed in Table 1. Maximum biosorption capacity of biosorbents (q_m) is found to be 35.7142 mg g-1 of tamarind pod shell (*Tamarindus indica* L.). The essential characteristics of the Langmuir isotherm parameters can be used to predict the affinity between the sorbate and sorbent using

$$R_L = \frac{1}{1+bC_i} \qquad (6)$$

Where b is the Langmuir constant and C_i is the maximum initial concentration of zinc (II). The value of separation parameters *RL* provides important information about the nature of adsorption. The value of *RL* indicated the type of Langmuir isotherm separation factor or dimensionless equilibrium parameters, *RL* expressed as in the following equation: to be irreversible (*RL* = 0), favorable (0 <*RL*< 1), linear (*RL* = 1) or unfavorable (*RL*>1). The *RL* was found to 0.1843 to 0.9186 for concentration of 5 mg/L-250 mg/L of zinc (II). They are in the range of 0-1 which indicates favorable biosorption (Malkoc and Nuhoglu 2005).
The freundlich (Freundlich, 1906) model is represented by the equation:

$$q = KC_e^{1/n} \qquad (7)$$

Where K and n are empirical constants incorporating all parameters affecting the adsorption process such as, sorption capacity and sorption intensity respectively. the Freundlich model was linearized as follows:

$$\log q = \log K + \frac{1}{n}\log C_e \qquad (8)$$

Equilibrium data for the adsorption is plotted as log q vs log Ce, as shown in Figure10 (b). The two constants n and K are calculated from the slope (1/n) and intercept (log K) of the line, respectively. The values of K, 1/n and regression coefficient (R^2) are listed in Table 1. The n value indicates the degree of non-linearity between solution concentration and adsorption as follows: if n = 1, then adsorption is linear; if n <1, then adsorption is chemical process; if n>1, then adsorption is a physical process. A relatively slight slope and a small value of 1/ n indicate that, the biosorption is good over entire range of concentration. The n value in Freundlich equation was found to be 1.1457. Since n<1, this indicates the chemical biosorption of zinc (II) onto tamarind pod shell (*Tamarindus indica* L.). The higher value of K (0.5842) indicates the higher adsorption capacity for the tamarind pod shell (*Tamarindus indica* L.).

Dubinin-Kaganer-Radushkevich (DKR) adsorption isotherm (Dubinin and Radushkevich, 1947):
The Dubinin Kaganer Radushkevich (DKR) adsorption isotherm (Santhi et al., 2010) model was also applied to estimate the porosity apparent free energy and the characteristics of adsorption. The D–R isotherm dose not assumes a homogeneous surface or constant adsorption potential. The D–R model has commonly been applied in the following Eq

$$lnq_e = \ln q_m - \beta\, \varepsilon^2 \qquad (9)$$

Where q_m is the maximum sorption capacity, β is the activity coefficient related to mean sorption energy and ε is the polanyi potential, which is calculated from the following relation:

$$\varepsilon = RTln\left(1 + \frac{1}{C_e}\right) \qquad (10)$$

Equilibrium data for the adsorption is plotted as lnq_e vs ε^2, as shown in Figure10 (c). The two constants β and q_m are calculated from the slope (β) and intercept (lnq_m) of the line, respectively. The values of adsorption energy E was obtained by the following relationship.

$$E = \frac{1}{\sqrt{-2\beta}} \qquad (11)$$

The E value was found to be 0.7071 KJ mol-1.The mean free energy gives information about biosorption mechanism whether it is physical or chemical biosorption. If E value lies between 8 KJ mol-1 and 16 KJ mol-1, the biosorption process take place chemically and E> 8 KJ mol-1, the biosorption process of the physical in nature (Olivieri and Brittenham, 1997). In the present work, E value (0.7071 KJ mol^{-1}) which is less than 8 KJ mol^{-1}, the biosorption of zinc (II) ions onto tamarind pod shell (*Tamarindus indica* L.) is of physical in nature (Sawalha et al., 2006).
Temkin adsorption isotherm (Temkin and Pyzhev, 1940):
The Temkin (Aharoni and Ungarish, 1977) isotherm has generally been applied in the following form:

$$q_e = \frac{RT}{b_T}\ln(A_T\, C_e) \qquad (12)$$

Where b_T is the Temkin constant related to heat of sorption (J/mol) and A_T is the Temkin isotherm constant (L/g).Equilibrium data for the adsorption is plotted as q_e vs lnCe, as shown in Figure 10(d). The two constants b_T and A_T are calculated from the slope (R_T/b_T) and intercept ($R_T/b_T \cdot \ln A_T$) of the line. The values of A_T, b_T and regression coefficient (R^2) are listed in Table 1. The various constants and regression coefficient R^2 obtained from adsorption an isotherm (Langmuir, Freundlich, Dubinin-KaganerRedushkevich (DKR) and Temkin) is summarized in Table 1.

The values of parameters and correlation coefficients for each isothermal model for zinc (II) biosorption with tamarind pod shell (*Tamarindus indica* L).

Langmuir parameters			Freundlich parameters			DKR parameters				Temkin parameters		
q_m	β	R^2	K	$1/n$	R^2	B	q_m	E	R^2	A_T	b_T	R^2
35.7142	0.0177	0.9898	0.5842	0.962	0.9983	-1E-06	12.5572	0.7071	0.6078	0.4118	311.379	0.8203

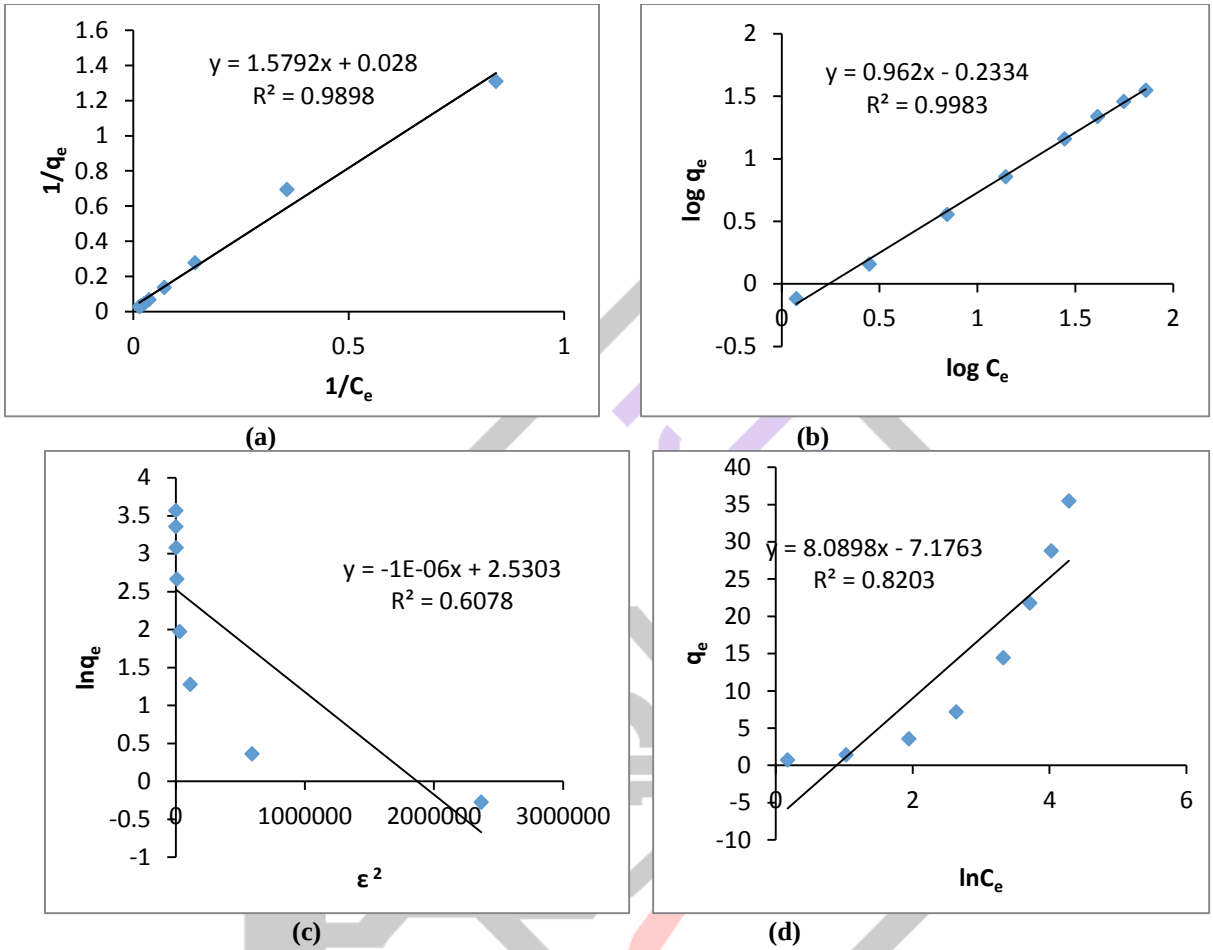

Figure10: Adsorption isotherm models (a) Langmuir, (b) Freundlich (c) DKR and (d) Temkin for biosorption of zinc (II) by tamarind pod shell (*Tamarindus indica* L.) (pH: 6.0, biosorbent dose concentration: 5 g/L, contact time: 120 minutes, temperature: 30^{0}C, agitation rate: 120 rpm)

Kinetic models

The study of adsorption kinetics is very useful for understanding the involved mechanisms and also for the design of future large scale adsorption facilities. Many models are used to fit the kinetic adsorption experiments. The most used ones are the pseudo-first order, pseudo-second order, intra-particle diffusion and Elovich models (Ozacar *et* al., 2004; Ornek *et* al., 2007). Equations are representing as,

$$\ln(q_e - q_t) = \ln q_e - k_1 t \quad (13)$$

$$\frac{t}{q_t} = \frac{1}{k_2 q_e^2} + \frac{t}{q_e} \quad (14)$$

$$q_t = \frac{1}{\beta}\ln(\alpha\beta) + \frac{1}{\beta}\ln t \quad (15)$$

$$q_t = k_i t^{0.5} + c \quad (16)$$

Where q_e (mg g^{-1}) is the solid phase concentration at equilibrium, q_t (mg g^{-1}) is the average solid phase concentration at time t (min), k_1 (min-1) and k_2 (g mg^{-1} min^{-1}) are the pseudo-first-order and pseudo-second-order rate constants, respectively. The symbols of α (mg g^{-1} min^{-1}) and β (g mg^{-1}) are Elovich coefficients representing initial sorption rate and desorption constants, respectively. k_i (mg g^{-1} min$^{-1/2}$) is the intra-particle diffusion rate constant, c is intercept.

If the adsorption follows the pseudo-first-order model, a plot of ln (q_e-q_t) against time t should be a straight line. Similarly, t/q_t should change lineally with time t if the adsorption process obeys the pseudo-second order model. If the adsorption process obeys Elovich model, a plot of qt against ln t should be a straight line. Also a plot of q_t against $t^{0.5}$ changes lineally the adsorption process obeys the Weber and Morris intra-particle diffusion model. Kinetic plots depicted in Figure 8 (a) (b) (c) and (d) (Septhum et al., 2007).

Biosorption of zinc (II) onto biosorbent was monitored at different specific time interval. The zinc (II) uptake was calculated from the data obtained. From the zinc (II) uptake was plotted against time to determine a suitable kinetic model, the adsorption data was fitted into pseudo-first-order model, pseudo-second-order model, Elovich models and the Weber & Morris intra-particle diffusion model.

The pseudo-first-order model was plotted for ln (q_e-q_t) against t (Figure 11 (a)). The values of k_1 and q_e values were calculated from the slope (k_1) and intercept (ln q_e) of the plot and shown in Table 2. Pseudo-first-order model showered the correlation value (R^2= 0.9258) being lower than the correlation coefficient for the pseudo-second-order model. Kinetic biosorption for pseudo-firstorder model occurs chemically and involves valency forces through ion sharing or exchange of electron between the biosorbent and the ions adsorbed onto it (Septhum et al., 2007).

The pseudo-second-order model was plotted for t/q_t against t (Figure 11 (b)). The values of q_e and k_2 are calculated from the slope (1/q_e) and intercept (1/k_2 q_e^2) of the plot and values are shown in Table 2. Pseudo-second-order kinetic model showered the strongest correlation (R^2= 0.9897). This suggests that zinc (II) biosorption occurs in a monolayer fashion and which relies on the assumption that chemisorption or chemical adsorption is the rate-limiting step. Zinc (II) reacts chemically with the specific binding sites on the surface of biosorbent.

The Elovich model was plotted for q_t against ln t (Figure 11 (c)). The values of β and α are calculated from the slope (1/ β) and the intercept (ln (α β)/ β) of the plot and values are shown in Table 2. The Elovich model showed a (R^2= 0.9497) being lower than the correlation coefficient for the pseudo-second-order model. The Elovich model has been used with the assumption that the actual Adsorption surface is energetically heterogeneous (Thomas and Thomas, 1997). The Weber & Morris intra-particle diffusion model was plotted for q_t against $t^{0.5}$ (Figure 11 (d)). The value of k_i and c are calculated from the slope (k_i) and intercept (c) of the plot and values are shown in Table 2. The Weber and Morris intra-particle diffusion model showed a (R^2= 0.9226) being lower than the correlation coefficient for the pseudo-second-order model. The intercept of the plot does not pass through the origin, this is indicative of some degree of boundary layer control and intraparticle pore diffusion is not only rate-limiting step (Weber and Morris, 1963). The plot of intra-particle diffusion model showed multilinearity, indicating that three steps take place. The first, sharper portion is attributed to the diffusion of adsorbate through the solution to the external surface of biosorbent or the boundary layer diffusion of solute molecules. The second portion describes ion stage, where intra-particle diffusion is a rate limiting. The third portion is attributed to the final equilibrium stage. However the intercept of the line fails to pass through the origin which may attribute to the difference in the rate of mass transfer in the initial and final stages of biosorption (Panday et al., 1986).

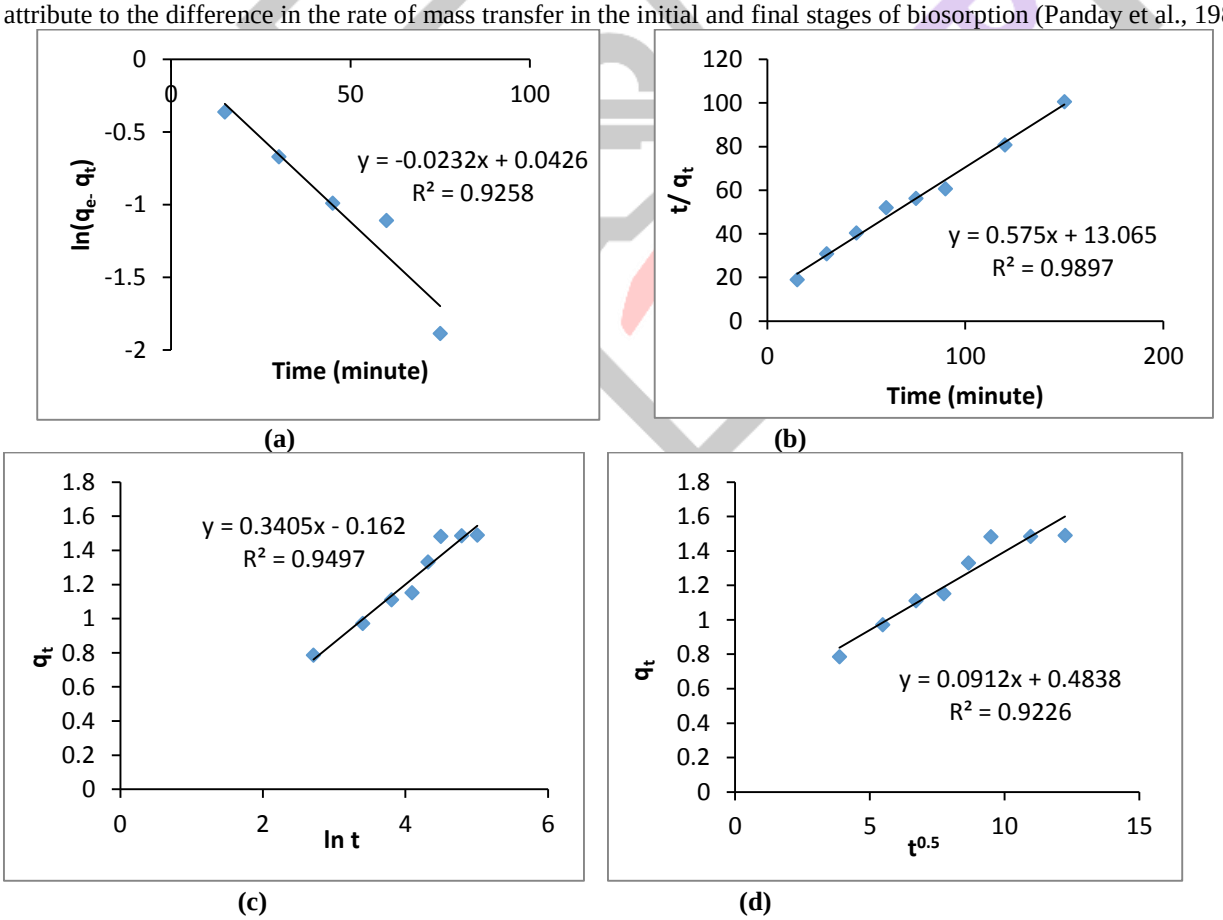

Figure 11: Adsorption kinetic models (a) pseudo-first-order model (b) pseudo-second-order model (c) Elovich model and (d) Weber and Morris intra-particle diffusion model, for biosorption of zinc (II) by tamarind pod shell (*Tamarindus indica*

L.) (pH: 6.0, biosorbent dose concentration: 5 g/L, initial zinc (II) concentration: 5 mg/L, temperature: 30^{0}C, agitation rate : 120 rpm)

Table 2. Kinetic parameter for the adsorption of zinc (II) onto Tamarind pod shell (*Tamarindus indica* L.)

Pseudo-first-order model			Pseudo-second-order model			Elovich model			Intraparticle diffusion model		
q_e	k_1	R^2	q_e	k_2	R^2	a	β	R^2	Ki	c	R^2
1.0435	0.0232	0.9258	1.7391	0.0253	0.9897	0.2116	2.9368	0.9497	0.0912	0.4838	0.9226

Thermodynamic

The effect of temperature on removal of zinc (II) from aqueous solutions in the concentration of zinc (II) 5 mg/L and biosorbent dose 5 g/l with optimum pH 6.0 was studied. Experiments were carried out at different temperatures from 20^{0}C to 40^{0}C. The samples were allowed to attain equilibrium. Sorption slightly increases from. The equilibrium constant (Catena and Bright, 1989) at various temperatures and thermodynamic parameters of adsorption can be evaluated from the following equations:

$$K_c = \frac{C_{Ae}}{C_e} \quad (17)$$

$$\Delta G^0 = -RT \ln K_c \quad (18)$$

$$\Delta G^0 = \Delta H^0 - T\Delta S^0 \quad (19)$$

$$lnK_c = \frac{\Delta S^0}{R} - \frac{\Delta H^0}{RT} \quad (20)$$

Where K_c is the equilibrium constant, Ce is the equilibrium concentration in solution (mg/L) and C_{Ae} is the amount of zinc (II) ions biosorbed on the biosorbent per liter of
solution at equilibrium (mg/L). ΔG^0, ΔH^0 and ΔS^0 are changes in Gibbs free energy (kJ/mol), enthalpy (kJ/mol) and entropy (J/mol K), respectively. R is the gas constant (8.314 J/mol K) and T is the temperature (K). The values of ΔH^0 and ΔS^0 were determined from the slope and the intercept from the plot of lnKc versus 1/T (Figure 12). The values of equilibrium constant (K_c), Gibbs free energy change (ΔG^0), enthalpy change (ΔH^0) and the entropy change (ΔS^0) calculated in this work were presented in Table 3. The equilibrium constant (K_c) increases with increase in temperature, which may be attributed to the increase in the pore size and enhanced rate of intra-particle diffusion. The Gibbs free energy (ΔG^0) is small and negative and indicates the spontaneous nature of the biosorption. The values of ΔG^0 were found to decreases as the temperature increases, indicating more driving force and hence resulting in higher biosorption capacity. The value of ΔH^0 was positive, indicating the endothermic nature of the biosorption of zinc (II) ions onto tamarind pod shell (*Tamarindus indica* L.). The positive values of ΔS^0 shows an affinity of biosorbent and the increasing randomness at the solid solution interface during the biosorption process.

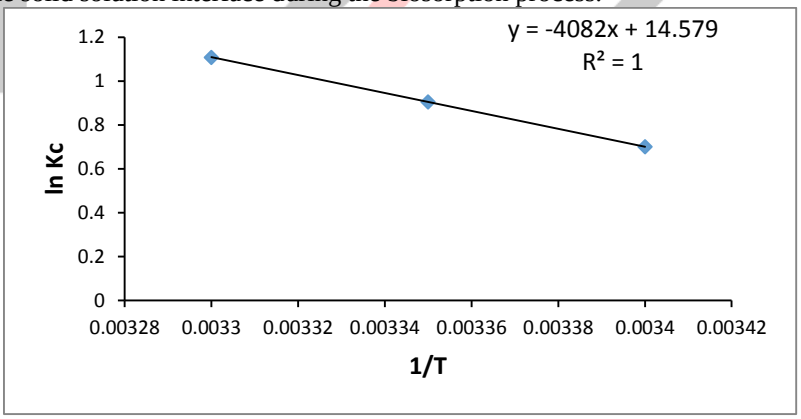

Figure 12: Plot of ln *Kc* against *1/T* for determination of thermodynamic parameters for biosorption of zinc (II) by tamarind pod shell (*Tamarindus indica* L.) (pH: 6.0, biosorbent dose concentration: 5 g/L, initial zinc (II) concentration: 5 mg/L, agitation rate: 120 rpm contact time: 120 minute).

Table 3: Thermodynamic parameters of zinc (II) biosorption onto tamarind pod shell (*Tamarindus indica* L.)

Sr. No.	Temperature (C^0)	Temperature (K)	$-\Delta G^0$	ΔH^0	ΔS^0
1	20^0C	293	1.7052	33.937	121.209
2	25^0C	298	2.2424		
3	30^0C	303	2.7917		
4	40^0C	313	2.7680		

Reference

Aharoni C, M Ungarish (1977). Kinetics of activated chemisorption Part 2. The oriental models, J. Chem. Soc. Faraday Trans. 73, pp. 456-464.

Bereket G, Aroguz AZ, Ozel MZ (1997). Removal of Lead, Cd(II), Cu(II), and Zn(II) from aqueous solutions by biosorption on bentonite. J. Colloid Interface Sci., 187, 338.

Bradl, H.: Heavy Metals in the Environment.1sted. London: Elsevier, 2005, pp. 282.

Carvalho de, R.P., K.H. Chong and B. Volesky, 1995 Evaluation of the Cd, Cu and Zn biosorption in two metal systems using an algal biosorbent. Biotechnology Progress, 11: 39-44.

Catena G. C. and Bright F. V., (1989). Thermodynamic study on the effect of cyclodixtrin inclusion with aniline naphthalene sulphonates. Anal. Chem., 61: 905-909.

Dostalek, P., M. Patzak and P. Matejka, (2004). Influence of specific growth limitation on biosorption of heavy metals by Saccharomyces cerevisiae. International Biodeterioration and Biodegradation 54: 203-207.

Drake, L.R. and G.D. Rayson (1996). Plant derived materials for metal ion selective binding and pre-concentration. Analytical Chemistry News and Features, 1: 22-27.

Dubinin M. M. and Radushkevich L. V. (1947). Equation of the characteristic curve of activated charcoal, Proc. Academy of Sci. Phy. Chem. Section, U.S.S.R., 55: 331-333.

Freundlich H. M. F., (1906).Uber dies adsorption in losungen, Zeitschriftfue Physikalische Chemie (Leipzig), A57: 385-470.

Gupta, V.K., Gupta, M. and Sharma, S., (2001). Water Res. 35(5):1125 – 134.
Gupta, V.K., Sharma, S. (2003) Removal of zinc from aqueous solutions using bagasse fly ash - a low cost adsorbent. Ind. Eng. Chem. Res., 42, 6619-6624.

Langmuir I., (1918). The adsorption of gases on plane surface of glass, mica and platinum, J. Am. Chem. Soc., 40: 1361-1403.

Macchi, G., D.D. Marconi and G. Tiravarthi (1986). Uptake of mercury by exhausted coffee grounds. Environ. Technol. Lett., 7: 431-444.

Malkoc E. and Nuhoglu Y. J., (2005). Investigation of Nickel (II) removal from aqueous solutions using tea factory waste, J. Hazard. Mater, B127: 120-128.

Mueler, M.D., D.C. Wolf, T.J. Beveridge an G.W. Bailay (1992). Sorption of heavy metals by thesoil fungi Aspergillus niger and Mucor rouxii. Soil Biology Biochemistry, 24: 129-135.

Naidu, R., R.S. Kookuna, D.P. Oliver, S. Rogers and M.J. Mc Laughlin (1996). Contaminants and the soil environment in the Austrilasia-Pacific Region. Proceedings of the First Australasia Pacific Conference on Contaminants and Soil Environment in the Australasia-Pacific Region, held in Adelaide, Kluwer Acedamic Publishers, pp. 629-646.

Olivieri N. F. and Brittenham G. M., (1997). Iron-chelating therapy and the treatment of thalassemia. Blood, 89: 739761.

Ornek A., Ozacar M., Sengil I. A., (2007) Adsorption of lead ontoformaldehyde or sulphuric acid treaed acorn waste: equilibrium and kinetic studies, Biochem. Eng. J. 37, pp. 192-200.

Ozacar M., Sengil I. A. (2004) Application of kinetic models to the sorption of disperse dyes onto alunite. Colloids Surf. A 242, pp. 105-113.

Panday K. K., Prasad G. and Singh V. N., (1986). Mixed adsorbents for Cu (II) removal from aqueous solutions. Environ. Technol. Lett., 50: 547-550.
Santhi T, S Manonmani, T Smitha (2010). Kinetics and isotherm studies on cationic dyes adsorption onto annona squmosa seed activated carbon" International journal of engineering science and technology, 2(3), 287-295.

Sawalha, M. F. and Peralta-Videa, J. R., Romero-Gonzalez, J. and Gardea-Torresdey, J. L., (2006). Biosorption of Cd (II), Cr (III) and Cr (VI) by saltbush (Atriplexcanescens) biomass: Thermodynamic and isotherm studies, J. Colloid Interface Sci., 300: 100-104.

Selatnia A., A. Boukazoula, N. Kechid, M.Z. Bakhti, A. Chergui, Y. Kerchich (2004). Biosorption of lead (II) from aqueous solution by a bacterial dead Streptomyces rimosus biomas. - Biochemical Engineering Journal, 19(2):127-135.

Septhum, C., Rattanaphani, S., Bremner, J. B. and Rattanaphani, V (2007). An adsorption of Al (III) ions onto chitosan. J. Hazardous Materials. 148, pp.185-191.

Temkin M. J. and Pyzhev V., (1940). Kinetics of ammonia synthesis on promoted iron catalysts. ActaPhysiochim. Urrs, 12: 217-222.

Thomas, J. M. And Thomas, W. J., (1997). Principle and Practice of heterogeneous catalysis, weinheim, VCH.

Weber W. J. and Morris J. C., (1963). Kinetics of adsorption on carbon solution. J.Sanit. Eng. Div. Am. Soc. Civ. Engg., 89: 31-59.